Mechanical restoration and failure analyses of a hydrogel and scaffold composite strategy for annulus fibrosus repair

Rose Long, Alexander Bürki, Philippe K Zysset, David Eglin, Dirk Grijpma, Sebastien B.G. Blanquer, Andrew Hecht, James Iatridis

HHS Public Access

Author manuscript

Acta Biomater. Author manuscript; available in PMC 2017 January 15.

Published in final edited form as:

Acta Biomater. 2016 January 15; 30: 116–125. doi:10.1016/j.actbio.2015.11.015.

Mechanical Restoration and Failure Analyses of a Hydrogel and Scaffold Composite Strategy for Annulus Fibrosus Repair

Rose G Long[1,4], **Alexander Bürki**[2], **Philippe Zysset**[2], **David Eglin**[3,4], **Dirk W. Grijpma**[4,5,6], **Sebastien BG Blanquer**[4,5], **Andrew C Hecht**[1], and **James C Iatridis**[*,1,4]

[1]Leni & Peter W. May Department of Orthopaedics, Icahn School of Medicine at Mount Sinai, New York, NY, USA [2]Institute for Surgical Technology & Biomechanics, University of Bern, Bern, Switzerland [3]AO Research Institute Davos, Davos, Switzerland [4]Collaborative Research Partner Annulus Fibrosus Rupture Program of AO Foundation, Davos, Switzerland [5]University of Twente, Department of Biomaterials Science and Technology, PO Box 217, 7500 AE Enschede, The Netherlands [6]University of Groningen, University Medical Centre Groningen, Department of Biomedical Engineering, PO Box 196, 9700 AD Groningen, The Netherlands

Abstract

Unrepaired defects in the annulus fibrosus of intervertebral discs are associated with degeneration and persistent back pain. A clinical need exists for a disc repair strategy that can seal annular defects, be easily delivered during surgical procedures, and restore biomechanics with low risk of herniation. Multiple annulus repair strategies were developed using poly(trimethylene carbonate) scaffolds optimized for cell delivery, polyurethane membranes designed to prevent herniation, and fibrin-genipin adhesive tuned to annulus fibrosus shear properties. This three-part study evaluated repair strategies for biomechanical restoration, herniation risk and failure mode in torsion, bending and compression at physiological and hyper-physiological loads using a bovine injury model. Fibrin-genipin hydrogel restored some torsional stiffness, bending ROM and disc height loss, with negligible herniation risk and failure was observed histologically at the fibrin-genipin mid-substance following rigorous loading. Scaffold-based repairs partially restored biomechanics, but had high herniation risk even when stabilized with sutured membranes and failure was observed histologically at the interface between scaffold and fibrin-genipin adhesive. Fibrin-genipin was the simplest annulus fibrosus repair solution evaluated that involved an easily deliverable adhesive

[*]Corresponding author: Dr. James C. Iatridis. Icahn School of Medicine at Mount Sinai, Dept. of Orthopaedics, One Gustave Levy Place, Box 1188, NY, NY 10029 USA; phone: 212-241-1517; james.iatridis@mssm.edu.

6. Disclosures

RGL: none
AB: none
PZ: none
DGE: none
DG: Consultant, co-founder and shareholder of Medisse BV
ACH: consultant and royalties from Zimmer Spine, surgical advisory board Zimmer Spine; consultant Medtronic Spine, editorial board of J. Spinal Disorders, Am J Orthopaedics, Spine Surgery Today, Orthopaedics Today
JCI: Grant funding as listed.

that filled irregularly-shaped annular defects and partially restored disc biomechanics with low herniation risk, suggesting further evaluation for disc repair may be warranted.

Keywords

annulus fibrosus repair; annular closure; intervertebral disc herniation; spine biomechanics; intervertebral disc degeneration

1. Introduction

Lower back pain affects up to 70% of people in their lifetimes [1] and is the leading cause of global disability [2,3]. Defects of the annulus fibrosus (AF) can result in herniation of intervertebral disc (IVD) material and compression of the nerve root, inducing back or leg pain. Discectomy is the most common and effective surgical procedure at reducing leg pain related to IVD herniation [4–6]. It consists of removing extruded and loose nucleus pulposus (NP) tissue through an incision in the AF. However, both small and large defects in the AF can lead to altered biomechanics and increased degeneration risk [7–10]. A systematic review of the discectomy literature indicated that discectomy procedures have up to 27% risk of re-herniation requiring further surgery, and the prevalence depends on the size of the annular defect and the amount of material removed [11,12]. There also remains a relatively high risk of degeneration and persistent low back pain in longer-term follow-up, particularly if excess IVD material was removed to lower the reherniation risk. While discectomy procedures are very effective at reducing leg pain, there are opportunities to improve this procedure with AF repair techniques that reduce the rate of reherniation, improve biomechanics and can potentially be part of a disc regeneration strategy.

Annular defects result in loss of NP pressurization and AF integrity. A functional AF repair strategy must restore IVD height, neutral zone characteristics, and torsional biomechanics to the healthy condition without risk of herniation under the high physiological loads occurring in the spine [8]. Current AF repair strategies include sutures, plugs, adhesives and hydrogels [13]. Suturing the IVD during a discectomy procedure adds substantial complications to the procedures and extends the operation time. Suturing did not restore the intradiscal pressure of IVDs with different annular defects in sheep [14], suggesting suturing alone provided inadequate biomechanical repair. An alternative to manual sutures was a commercially available suture delivery system, the Xclose Tissue Repair System (Anulex Technologies, Minnetonka, MN). The Xclose device was designed to strengthen the suturing procedure and simplify the suturing process via an elongated suture delivery system allowing arthroscopic access. In a two year prospective, randomized control trial there was no difference in functional or disability outcomes between microdiscectomy performed with and without XClose sutures, although there was a significant reduction in re-herniation surgery observed in a subset cohort with predominant leg pain at 3 and 6 months [15]. The reduction in re-herniation rates was promising for a sutured AF repair, but no data was reported on disc height, biomechanical restoration of the motion segment, or MRI signal intensity providing no evidence that this technique would successfully prevent accelerated degeneration following discectomy procedures. An annulus closure plug had favorable biomechanical results in vitro but showed deformation and herniation after 6 weeks in an in

vivo goat model [16]. Alternately, Barricaid is a device resembling a shield that is secured with an anchor into the adjacent inferior vertebral body to reduce the risk of tissue expulsion following a discectomy procedure (Intrinsic Therapeutics, Inc., Woburn, MA). In an in vitro test of 6 IVDs, no herniation was seen after more than 100,000 cycles of dynamic bending, indicating a low risk of herniation, however, the IVD height loss due to loading was not decreased [17] indicating limited biomechanical restoration. Barricaid demonstrated a reduced risk of facet degeneration [18], suggesting AF repair strategies capable of retaining NP pressurization following discectomy are likely to have improved outcomes. While several mechanical annular repair strategies exist, they all complicate discectomy procedures, several have risk of herniation, and none completely restore IVD biomechanics.

The broad aim of this study was to evaluate the repair of large AF defects using a composite repair strategy involving fibrin-genipin (FibGen) hydrogel adhesive to seal the AF defect, a poly(trimethylene carbonate) (PTMC) space-filling scaffold capable of cell delivery, and a polyurethane membrane to prevent herniation. Design criteria we considered necessary for an effective AF repair strategy included low risk of herniation, restoration of IVD biomechanics to the healthy (intact) condition, ease of delivery, and the potential to be functionalized to deliver cells or drugs in order to promote long-term healing or regeneration. This three part biomechanical study assessed the performance of multiple composite repair strategies using these components evaluated under multiple degree of freedom biomechanical testing using bovine caudal IVD injury models. Part 1 applied a torsional stiffness test to evaluate whether the repair restored AF integrity since mechanical integrity of annulus fibrosus integrity is most sensitive to torsion [9,19]. Part 1 tested the hypothesis that the composite repair strategy with scaffolds would best restore biomechanics to intact levels but the adhesive alone would have the lowest herniation risk. Part 2 selected the most promising repairs from Part 1 and after procedure refinement, evaluated them for herniation risk and biomechanical restoration in axial compression and two bending degrees of freedom. Bending was evaluated since it can rigorously test for herniation risk. Part 2 tested the hypothesis that the FibGen adhesive alone and the composite repair with suturing augmentation could restore biomechanics and disc height loss without risk of herniation. Part 3 used the most successful repair strategies from Parts 1 & 2 and evaluated mechanical restoration using a cruciate-style defect to be more representative of the variety of defects found clinically following herniation and discectomy procedures[12] (rather than biopsy defects) and to evaluate if FibGen could adhere to irregularly-shaped defects. Part 3 used an angle control with moment limits test. in 3 rotational degrees of freedom (i.e., torsion, flexion-extension & lateral bending). Part 3 was performed at the University of Bern (rather than Mount Sinai). Part 3 tested the hypothesis that the FibGen can seal a cruciate-style defect and restore the biomechanical behaviors to intact levels in bending, flexion-extension, and axial rotation.

2. Materials and Methods

2.1 Material selection

FibGen involved a genipin-crosslinked fibrin gel with a formulation previously tuned to match the shear properties of the native AF tissue [20]. The space filling PTMC scaffolds

consisted of 5,000g/mol oligomers crosslinked with stereolithography to ensure a precise structure that mimicked the complex architecture of the AF collagen bundles which are oriented in an angle-ply fashion that evolve from ±30° in the inner AF to ±45° in the outer AF[21]. Two scaffold geometries were evaluated: a truncated cone shape and a cylindrical shape. A polyurethane membrane was designed to prevent extrusion of IVD tissue and provide a barrier between the IVD and the adjacent sensitive nerve. The polyurethane membrane was adhered to the native AF tissue using FibGen adhesive as well as suturing.

2.2 Animal model, dissection and storage

Bovine coccygeal IVDs are large and comparable to human lumbar IVD [22,23], easily available and well-studied. Motion segments (bone-IVD-bone) were harvested from skeletally mature bovine tails obtained from a local abattoir (Green Village Packing, Green Village, NJ). Following dissection, IVDs were wrapped in saline soaked tissue and frozen at −20°C until testing. On the day of testing, all specimens were thawed for 3 hours in 1L PBS at 37°C and warm to touch, then potted in polymethylmethacrylate (PMMA). No discs underwent additional freeze-thaw cycles in order to decrease the change in biomechanics due to freeze-thaw cycles [24]. To minimize variability in injury and repair procedures, a single biomedical engineer performed injury and repair procedures for each Part (as described in Sections 2.3–2.5) following training by a spine surgeons and extensive practice on all techniques.

2.3 Part 1: Biomechanical restoration and herniation risk in torsion of three repair strategies

Thirty bovine coccygeal IVDs were distributed to five groups (n=6): Intact, Injured, FibGen, Cylindrical (scaffold), and Conical (scaffold) (Figure 1).

The Intact specimens did not have a defect. The Injured group had a 5 mm biopsy punch defect through the posterolateral AF with removal of approximately 30% of the nucleus pulposus (173±84 mg) with rongeurs. In the FibGen group, the injury was repaired by filling the defect with FibGen adhesive and covering the FibGen with the polyurethane membrane. The Cylindrical group specimens were repaired by filling the defect partially with FibGen adhesive and inserting a cylindrical scaffold (diameter=5 mm, length=7 mm). The Cylindrical scaffold was designed to match the width of the bovine annulus fibrosus which is about 5 mm[25]. The porous scaffold was filled with FibGen and covered with membrane cut into a circle (diameter=8 mm). The Conical group was prepared identically to the Cylindrical group but involved a scaffold with a truncated cone shaped scaffold (diameter= 4/6 mm, length 10 mm) with the larger diameter to be seated at the innermost portion of the AF to create a press-fit, and was longer than the Cylindrical scaffold since it was designed to be seated within the nucleus pulposus. For all the repair groups, the FibGen adhesive was prepared as previously described [20]. Briefly, 40.5 μL of thrombin (100 U/mL) was mixed with 20.25 μL of genipin (400 mg/mL in DMSO) and 226.8 mL PBS. This was mixed 1:4 with fibrinogen (200 mg/mL) upon injection using a dual barrel syringe with mixing tip.

All specimens were submerged in PBS with protease inhibitor (cOmplete, Roche Diagnostics, Indianapolis, IN, USA) and allowed to set at 37°C overnight before testing.

Specimens were tested using a Bionix Servohydraulic system (MTS, Eden Prairie, MN, USA) capable of one translational and three rotational degrees of freedom. Each specimen was subjected to several rounds of rotations of 20 cycles each, increasing incrementally from physiological to hyper-physiological levels (±19°) at 0.1 Hz with axial displacement fixed after a 60 N preload in compression was applied (Figure 1) to allow identification of rotations and loads that induced herniation. Herniation was monitored with a camera throughout the loading and was defined by extrusion of the repair beyond the surface of the IVD. Torque range and torsional stiffness were calculated using custom Matlab (Mathworks, Natick, MA, USA) code with the torque range calculated as the total torque developed in the 2nd to last cycle of each round and torsional stiffness calculated as the average of the top 10% rotation of both loading directions. Torsional stiffness and torque range were calculated for each sample until the end of the test and only presented up to the point of extrusion. Herniation was observed visually with photography, and in most samples (75%), was coincident with an abrupt reduction of axial force, indicating a loss of nucleus pressurization. The torque, rotation and nominal axial stress at herniation were measured. Nominal axial stress was calculated as the maximum axial force just before herniation divided by undeformed cross-sectional area of the IVD. This nominal axial stress was developed as a reactive stress due to applied compression, fixing of the disc height and applied torsion. While failure occurred due to excess torsion, these values were calculated to give an indication of the nominal axial stress when that failure occurred during torsional loading.

2.4 Part 2: Biomechanical restoration and herniation risk prevention in bending of two repair strategies

Part 2 was designed to test herniation behaviors and herniation prevention of refined repairs using a repeated measures study design with three groups: Injured, Conical and FibGen (n=6) (Figure 2). Part 2 repairs were improved from Part 1 repairs by the following: i) the membrane over the Large Scaffold repair was cut to be square-shaped to allow suturing, one at each corner, in order to better prevent expulsion and herniation of the scaffold; and ii) the FibGen repair did not have a membrane since it was considered unnecessary due to low risk of herniation and minimal contribution of the membrane observed in Part 1.

Each specimen was subjected to a moderate loading protocol in Intact, Defect and Repaired conditions (Figure 2). Specimens were x-rayed to evaluate orientation, alignment and IVD height to ensure centrality with respect to the circular pots and alignment with the cephalocaudal axis. Diameter was found by averaging four caliper measurements at different locations around the disc assuming a circular cross-section. The IVD height was calculated using a custom written Matlab (Mathworks, Natick, MA, USA) code that averaged the distance between cubic functions fit to each endplate. The moderate loading protocol consisted of twenty cycles each of compression from 0.06 MPa to 0.50 MPa at 0.1 Hz, and off injury axis and on injury axis bending to ±8° at 1.5°/sec (Figure 2). The nominal axial stress of 0.50 MPa was chosen because it approximates sitting [26,27] and would represent the axial loading the repair must withstand after a discectomy procedure. The ±8° bending amplitude falls within the human lumbar motion segment physiological ranges of 8–13° in flexion, 1–5° in extension, and 3–11° in lateral bending [28–32]. Force, displacement,

torque and rotation around each axis were recorded through the test. IVD height change was calculated by dividing displacement at the end of the loading by the baseline IVD height determined with a pretest x-ray. Torque range was calculated as the total torque developed in the full range of bending in the 2nd to last cycle to allow for viscoelastic equilibrium [33]. The dynamic stiffness was calculated as the slope of a line fit to the final 20% deformation of the force-deformation curve and torque-rotation curve in each loading direction so as to approximate the linear region. The stiffnesses of each loading direction for both bending regimes were averaged. The defect and repaired condition stiffness values were normalized against the matching intact condition. After the last moderate testing cycle, the non-herniated specimens (6 FibGen & 1 Conical) were subjected to one of two rigorous testing protocols. The first 3 FibGen samples underwent a high magnitude failure test where on injury axis bending magnitude was increased successively to specimen failure. However, the test machine load cell limit (±10 Nm) was reached as bending angles reached ~±10.5° without observing any FibGen herniation. As a result, the remaining samples (3 FibGen & 1 Conical) underwent a rigorous cyclic failure test consisting of 2 hours of on injury axis bending to ±8° at 5°/sec resulting in ~1000 cycles. Herniation was monitored visually with photography.

All samples were fixed for histological analysis following testing. The failure mode of the repair was also assessed by imaging the interface between the repair and the native tissue using methacrylate embedded specimens histological sections with Picrosirius Red/Alcian Blue staining under brightfield microscopy as described [34,35].

2.5 Part 3: Biomechanical restoration in pure bending of FibGen with cruciate defect

Part 3 was designed to test mechanical restoration under a repeated measures flexibility test protocol with samples tested in three rotational degrees of freedom under three conditions: Intact, Injured and Repaired (n=7) (Figure 3). Important differences from Part 2 testing involved: i) a flexibility test was used in order to allow greater rotational motion; ii) a different and clinically relevant cruciate-style discectomy defect was used; and iii) testing was performed at the Institute for Surgical Technology and Biomechanics at the University of Bern. The cruciate injury was created using a No. 11 scalpel blade with a depth of approximately 8mm. The FibGen repair was allowed to set for four hours instead of overnight in order to approximate the timing of the first movement of a patient. The membrane was an octagon shape measuring about 15mm×15mm with no suture.

Samples were tested in intact, injured, and repaired conditions. The test consisted of three cycles in flexion-extension, lateral bending and torsion at a constant angular motion of 1°/s up to a torque limit of 1.5 Nm or a rotation limit of 20°. No axial compression was added (Figure 3). The moment and rotation were recorded through time. The range of motion (ROM) was calculated as the angular motion within the load range of ±1.5 Nm for flexion-extension and torsion and ±0.5 Nm for lateral bending during the third loading cycle (Figure 3).

2.6 Statistical Analysis

For Part 1, a Kruskal-Wallis test (non-parametric 1-way ANOVA) with Dunn's Multiple Comparison test was used to compare the torque range and stiffness between the groups and differences between nominal axial stress, maximal rotation and maximal torque. In Part 2, a Friedman's test (non-parametric, repeated-measure ANOVA) with Dunn's Multiple Comparison Test was used to compare the torque range and compressive and bending stiffness ratios between the three groups. The Friedman's test with Dunn's Multiple Comparison testwas used to test the effect of the injury on disc height loss compared to matched intact samples of all groups (n=18) and to test the effect of repair compared to matched injured samples within each treatment group (n=6). In Part 3, Friedman's test (non-parametric, repeated-measures ANOVA) with Dunn's Multiple Comparison test was used to compare the ratios of injured/intact to repaired/intact. All quantitative data are presented as mean ± standard deviation. Significance was based on $\alpha = 0.05$ level and all statistical analysis was performed using GraphPad Prism v. 5 (GraphPad Software, San Diego, California, USA).

3. Results

3.1 Part 1 Results: All repair groups partially restored biomechanics and FibGen had low herniation risk

All repair groups had stiffness and torque range values that were not different than the intact condition, suggestive of partial restoration to intact levels although injured was not significantly different than intact either (Figure 4B). The Intact group exhibited a shift in the shape of the Torsional Stiffness-Angle curve at 19°, and this may reflect injury initiation. No significant differences in torque range were detected between the repaired, intact and and injured group (Figure 4C).

As torsion angles increased, the repairs of the Conical and Cylindrical groups herniated, as demonstrated with an abrupt drop in nominal axial stress (Figure 5A). Herniation occurred for 100% of the Cylindrical scaffold and 83% of the Conical scaffold herniating compared to just 33% of the FibGen group. The FibGen group repairs withstood higher average rotations, torques and nominal axial stresses than either the Cylindrical or Conical groups, but this was only significant compared to the Conical group for max rotation (Figure 5B). No difference in the average maximum torque or nominal axial stress was observed between the Cylindrical, Conical and FibGen groups. Due to the slightly greater biomechanical restoration of the Conical scaffold group and lowest herniation risk of the FibGen group, both FibGen and Conical scaffold groups were retained and refined for Part 2 biomechanical evaluations.

3.2 Part 2 Results: FibGen had low herniation risk in compression and bending while Conical Scaffold had high herniation risk

FibGen repair showed low risk of herniation in bending and compression with no samples herniating in moderate or rigorous testing. The scaffold repair had a high risk of herniation with 5 out of 6 samples herniating during the moderate testing procedure (Figure 6B) and 1 sample herniating during the rigorous testing. Rigorous testing involved rotation angles of

10.7±4.7° on-axis bending for the high magnitude failure tests and ~1000 cycles of ±8° on-axis bending for the cyclic failure tests. The FibGen repair significantly reduced the disc height loss during moderate loading compared to matched Intact and Defect conditions. The disc height loss of the Conical repair group was not significantly different than the matched Intact and Defect conditions (Figure 6C), likely due to the high rate of observed herniation of the scaffold. There was no significant change in torque range, or bending and compressive stiffness ratios between the three groups.

The mechanism for scaffold extrusion was observed on histology to be failure between the FibGen and the PTMC scaffold for the scaffold groups (Figure 6A). FibGen remained adhered to the AF tissue, although FibGen showed some cracking on histology when observed after undergoing rigorous loading that also appeared to induce cracks in the native disc tissue.

3.3 Part 3 Results: FibGen partially restored biomechanical behaviors without herniation in bending flexibility tests

The cruciate-style AF injury resulted in significantly increased ROM compared to the Intact condition in flexion-extension, lateral bending and torsion with mean increases of 5.7%, 4.0% and 17.1%, respectively (Figure 7B–D). The FibGen repair restored the ROM to values significantly lower than Injured levels in flexion-extension and not significantly different than Intact levels in lateral bending. For torsion, FibGen did not decrease ROM from the injured condition to intact levels, consistent with the incomplete restoration of torque range in torsion seen in Part 1.

4. Discussion

A successful AF repair strategy remains an important unmet clinical need, and has the potential to reduce long-term degeneration following herniation and discectomy procedures. This comprehensive biomechanical study evaluated multiple AF repair strategies using FibGen, an adhesive sealant, a PTMC space-filling scaffold capable of delivering cells, and a polyurethane membrane designed to prevent herniation. A 3-part biomechanical study was performed involving distinct repair configurations, defects, and loading conditions in order to robustly assess if these materials could meet our design criteria. Part 1 found all repair strategies had values for torsional stiffness and torque range that were greater than injured but lower than intact groups, although there were minimal differences between repair groups and no groups had significant differences. FibGen had little herniation risk and the Conical scaffold group had the largest values for torsional stiffness so both repair strategies underwent continued evaluation in Part 2 studies, however, the conical scaffold repair was refined by adding sutures to the membrane to better prevent herniation. In Part 2, FibGen significantly reduced disc height loss and had the greatest values for compression stiffness ratio and both axes of bending stiffness ratio, although this was not significant. The Conical scaffold retained a high herniation risk even with the sutured membrane so was not used for further evaluation. In Part 3, FibGen adhesive filled the irregularly shaped cruciate-style defects and ROM values were lower than the Injured condition for all degrees of freedom, and this was significant for flexion-extension.

FibGen was demonstrated to be capable of filling cylindrical and cruciate-style AF defects. FibGen reduced IVD height loss and partially restored biomechanical behaviors of injured IVDs in multiple loading degrees of freedom, specifically flexion-extension ROM in bending and disc height loss after compression and bending. FibGen had little herniation risk and herniated only in some samples and only at hyper-physiological rotation angles. FibGen was also previously demonstrated to have surgically relevant gelation times of about 15 minutes[add guterl et al 2013]. The FibGen formulation in this study was tuned to mechanically match AF shear behaviors of the AF[36], but this isotropic hydrogel is unlikely to additionally match tensile and compressive behaviors of the anisotropic and fiber-reinforced AF. As a result, it is not surprising that torsional biomechanical behaviors were not completely restored to the intact condition. Furthermore FibGen remained adhered to the tissue and some evidence of FibGen cracking was observed on histology following rigorous loading. Therefore, FibGen enhancements to increase failure strength are suggested by this data to improve biomechanical performance. However, FibGen was previously shown to allow cell integration in vitro and in vivo and had degradation rates that were much longer than fibrin, suggesting potential for repair [20,36,37]. It is not possible to determine if the current formulation of FibGen is sufficient without future in vivo testing.

PTMC scaffold groups exhibited non-significant increases in torsional stiffness of the injured IVD although herniation occurred well within physiological ROM, which is less than approximately ±4° since rotation is limited by the facet joints [30,32,38]. Histology demonstrated failure occurred between the FibGen and PTMC scaffold so that FibGen adhesive did not adequately adhere to the scaffolds. The high rate of herniation observed for both scaffold geometries was likely due the hydrostatic pressure of the nucleus pushing the scaffold outward creating high shear stresses at the interface between the scaffold and FibGen. The polyurethane membrane was not sufficient to prevent scaffold expulsion under loading even when reinforced with sutures. The sutured polyurethane membrane in this study was visually observed to stretch and allowed the scaffolds to extrude even at low physiological loading levels. Consequently, it is unlikely that improved suturing methods (e.g., the Xclose Tissue Repair System which can tighten suture knots and reduce risks associated with suturing in close proximity to neural structures) would sufficiently reduce the high herniation risks. Furthermore, the Barricaid system has been shown to prevent NP herniation during rigorous biomechanical testing [17], and could be a useful augmentation to resist NP pressurization and reduce herniation risk of AF repair biomaterials described. Future optimization of the PTMC formulation, scaffold structure, and scaffold repair strategies that better prevent herniation are required, and additional optimization may be warranted since organ culture results indicate that activating the scaffold with human bone marrow derived mesenchymal stromal cells resulted in upregulation of anabolic genes and down regulation of catabolic genes[39].

Different test groups and loading conditions were used in Parts 1–3 due to the evolving refinements and demands of the AF repair strategies. However, not all biomaterials were able to be compared separately and some factors may interact preventing conclusions on specific biomechanical roles of each biomaterial component. For example, FibGen was not always evaluated with and without a membrane and the different scaffold geometrics differed in shape and length. The lack of significant effects of injury on torsional stiffness

and torque range in Part 1 may be due to the inter-animal differences in biomechanics since torsion is commonly reported to be strongly affected by AF injury [2,3,9,19]. This study used n=6, 6 & 7 for Parts 1, 2 & 3, respectively, so there is limited statistical power on some of the tests to detect smaller effects. Results demonstrated that the stiffness and the torque range of the repaired specimens in Part 1 were higher than injured condition and lower than intact condition, but not significantly, suggestive of reliable but insignificant pattern. Inter-specimen variability was reduced with repeated measures study designs in Parts 2 & 3. While there is likely to be an effect of loading history, it does not influence our conclusions since our conclusions are between groups with a repeated measures design and the same loading history for all groups. No significant effects of injury were detected in Part 2 which we attribute to the limited nucleus pulposus tissue removal which more rigorously induced implant failure but also likely retained tension in the surrounding AF fibers that were not injured. However, significant effects of injury were detected in Part 3 studies. The Part 1 & 2 tests tested herniation risk at greater bending and torsion angles than the commonly reported rigorous eccentric loading test of Heuer and colleagues [40], although our testing involved far fewer loading cycles and fatigue loading experiments is a relevant future investigation.

5. Conclusions

Discectomy procedures are highly effective at addressing acute pain due to herniation, yet risks of accelerated degeneration, reherniation, and diminished long-term success rates indicate there is an unmet clinical need for an effective AF repair strategy. An ideal AF repair strategy must have a low herniation risk, restore IVD biomechanics, and be easily deliverable during surgical procedures. Of the repair strategies evaluated in this study FibGen best met these design criteria because it had low herniation risk and was easily deliverable, but FibGen only partly restored disc biomechanical behaviors. The PTMC scaffold and polyurethane membrane had attractive design characteristics for AF repair, but when used as part of a composite repair strategy, FibGen was not sufficiently strong to prevent herniation of the PTMC scaffold even when reinforced by a sutured polyurethane membrane. Additional repair strategy development and biomaterial optimizations are required to prevent herniation of the PTMC scaffold and improve biomechanical performance of FibGen. However, complete biomechanical performance may not be necessary for IVD repair, and future large animal studies may be warranted to determine if FibGen can remain in place and adequately seal the IVDs under high levels of spinal loading in vivo until the AF can sufficiently repair itself.

Acknowledgments

The research reported in this publication was supported by grants from the National Institute of Arthritis and Musculoskeletal and Skin Diseases (R01AR057397) and National Institute of General Medical Sciences; Traineeship (T32 GM062754) of the National Institutes of Health and a Collaborative Research Partner Program grant on Annulus Fibrosus Rupture from the AO Foundation, Davos, Switzerland. The authors gratefully acknowledge the technical contributions and helpful discussions from Keegan Cole, Sarah Elsharkawy, Dr. Stephen Ferguson, Warren Hom, Damien Laudier, Diana Litsas, and Dr. Morakot Likhitpanichkul, Philip Nasser, Carine Rognon.

The providers of financial support for this study had no involvement: in the conduct of the research and/or preparation of the article; in study design; in the collection, analysis and interpretation of data; in the writing of the report; and in the decision to submit the article for publication.

Abbreviations

AF	annulus fibrosus
IVD	intervertebral disc
NP	nucleus pulposus
FibGen	genipin-crosslinked fibrin gel
PTMC	poly(trimethylene carbonate)
PMMA	polymethylmethacrylate
PBS	phosphate buffered saline
DMSO	Dimethyl sulfoxide
ROM	range of motion

References

1. Andersson GB. Epidemiological features of chronic low-back pain. Lancet. 1999; 354:581–5. [PubMed: 10470716]
2. Vos T, Flaxman AD, Naghavi M, Lozano R, Michaud C, Ezzati M, Shibuya K, Salomon JA, Lopez AD, Murray CJ, et al. Years lived with disability (YLDs) for 1160 sequelae of 289 diseases and injuries 1990–2010: a systematic analysis for the Global Burden of Disease Study 2010. Lancet. 2012; 380:2163–96. [PubMed: 23245607]
3. March L, Smith EUR, Hoy DG, Cross MJ, Sanchez-Riera L, Blyth F, Buchbinder R, Vos T, Woolf AD. Burden of disability due to musculoskeletal (MSK) disorders. Best Practice & Research Clinical Rheumatology. 2014; 28:353–66. [PubMed: 25481420]
4. Asch HL, Lewis PJ, Moreland DB, Egnatchik JG, Yu YJ, Clabeaux DE, Hyland AH. Prospective multiple outcomes study of outpatient lumbar microdiscectomy: should 75 to 80% success rates be the norm? J Neurosurg. 2002; 96:34–44. [PubMed: 11795712]
5. Weinstein JN, Lurie JD, Tosteson TD, Tosteson ANA, Blood EA, Abdu WA, Herkowitz H, Hilibrand A, Albert T, Fischgrund J. Surgical versus nonoperative treatment for lumbar disc herniation: four-year results for the Spine Patient Outcomes Research Trial (SPORT). Spine. 2008; 33:2789–800. [PubMed: 19018250]
6. Gray DT, Deyo RA, Kreuter W, Mirza SK, Heagerty PJ, Comstock BA, Chan L. Population-based trends in volumes and rates of ambulatory lumbar spine surgery. Spine. 2006; 31:1957–63. discussion1964. [PubMed: 16924213]
7. Elliott DM, Yerramalli CS, Beckstein JC, Boxberger JI, Johannessen W, Vresilovic EJ. The effect of relative needle diameter in puncture and sham injection animal models of degeneration. Spine. 2008; 33:588–96. [PubMed: 18344851]
8. Iatridis JC, Nicoll SB, Michalek AJ, Walter BA, Gupta MS. Role of biomechanics in intervertebral disc degeneration and regenerative therapies: what needs repairing in the disc and what are promising biomaterials for its repair? The Spine Journal. 2013; 13:243–62. [PubMed: 23369494]
9. Michalek AJ, Iatridis JC. Height and torsional stiffness are most sensitive to annular injury in large animal intervertebral discs. The Spine Journal. 2012; 12:425–32. [PubMed: 22627276]
10. Masuda K, Aota Y, Muehleman C, Imai Y, Okuma M, Thonar EJ, Andersson GB, An HS. A novel rabbit model of mild, reproducible disc degeneration by an anulus needle puncture: correlation between the degree of disc injury and radiological and histological appearances of disc degeneration. Spine. 2005; 30:5–14. [PubMed: 15626974]

11. McGirt MJ, Eustacchio S, Varga P, Vilendecic M, Trummer M, Gorensek M, Ledic D, Carragee EJ. A prospective cohort study of close interval computed tomography and magnetic resonance imaging after primary lumbar discectomy: factors associated with recurrent disc herniation and disc height loss. Spine. 2009; 34:2044–51. [PubMed: 19730212]
12. Watters WC, McGirt MJ. An evidence-based review of the literature on the consequences of conservative versus aggressive discectomy for the treatment of primary disc herniation with radiculopathy. The Spine Journal. 2009; 9:240–57. [PubMed: 18809356]
13. Guterl CC, See EY, Blanquer SBG, Pandit A, Ferguson SJ, Benneker LM, Grijpma DW, Sakai D, Eglin D, Alini M, Iatridis JC, Grad S. Challenges and strategies in the repair of ruptured annulus fibrosus. Eur Cell Mater. 2013; 25:1–21. [PubMed: 23283636]
14. Ahlgren BD, Lui W, Herkowitz HN, Panjabi MM, Guiboux JP. Effect of anular repair on the healing strength of the intervertebral disc: a sheep model. Spine. 2000; 25:2165–70. [PubMed: 10973397]
15. Bailey A, Araghi A, Blumenthal S, Huffmon GV. Prospective, Multicenter, Randomized, Controlled Study of Anular Repair in Lumbar Discectomy. Spine. 2013; 38:1161–9. [PubMed: 23392414]
16. Bron JL, van der Veen AJ, Helder MN, van Royen BJ, Smit TH, Skeletal Tissue Engineering Group Amsterdam, Research Institute MOVE. Biomechanical and in vivo evaluation of experimental closure devices of the annulus fibrosus designed for a goat nucleus replacement model. Eur Spine J. 2010; 19:1347–55. [PubMed: 20401620]
17. Wilke H-J, Ressel L, Heuer F, Graf N, Rath S. Can prevention of a reherniation be investigated? Establishment of a herniation model and experiments with an anular closure device. Spine. 2013; 38:E587–93. [PubMed: 23429676]
18. Trummer M, Eustacchio S, Barth M, Klassen PD, Stein S. Protecting facet joints post-lumbar discectomy: Barricaid annular closure device reduces risk of facet degeneration. Clin Neurol Neurosurg. 2013; 115:1440–5. [PubMed: 23473658]
19. Michalek AJ, Funabashi KL, Iatridis JC. Needle puncture injury of the rat intervertebral disc affects torsional and compressive biomechanics differently. Eur Spine J. 2010; 19:2110–6. [PubMed: 20544231]
20. Guterl CC, Torre OM, Purmessur D, Khyati D, Likhitpanichkul M, Hecht AC, Nicoll SB, Iatridis JC. Characterization of Mechanics and Cytocompatibility of Fibrin-Genipin Annulus Fibrosus Sealant with the Addition of Cell Adhesion Molecules. Tissue Eng Part A. 2014; 20:140506130038007.
21. Blanquer SBG, Sharifi S, Grijpma DW. Development of poly(trimethylene carbonate) network implants for annulus fibrosus tissue engineering. Jabfm. 2012; 10:177–84. [PubMed: 23242873]
22. Demers CN, Antoniou J, Mwale F. Value and limitations of using the bovine tail as a model for the human lumbar spine. Spine. 2004; 29:2793–9. [PubMed: 15599281]
23. Oshima H, Ishihara H, Urban JP, Tsuji H. The use of coccygeal discs to study intervertebral disc metabolism. Journal of Orthopaedic Research. 1993; 11:332–8. [PubMed: 8326439]
24. Tan JS, Uppuganti S. Cumulative multiple freeze-thaw cycles and testing does not affect subsequent within-day variation in intervertebral flexibility of human cadaveric lumbosacral spine. Spine. 2012; 37:E1238–42. [PubMed: 22660554]
25. O'Connell GD, Vresilovic EJ, Elliott DM. Comparison of animals used in disc research to human lumbar disc geometry. Spine. 2007; 32:328–33. [PubMed: 17268264]
26. Wilke HJ, Neef P, Caimi M, Hoogland T, Claes LE. Wilke 1999 New in vivo measurements of pressures in the intervertebral disc in daily life. Spine. 1999; 24:755–62. [PubMed: 10222525]
27. Sato K, Kikuchi S, Yonezawa T. In vivo intradiscal pressure measurement in healthy individuals and in patients with ongoing back problems. Spine. 1999; 24:2468–74. [PubMed: 10626309]
28. Lee S-H, Daffner SD, Wang JC. Does lumbar disk degeneration increase segmental mobility in vivo? Segmental motion analysis of the whole lumbar spine using kinetic MRI. J Spinal Disord Tech. 2014; 27:111–6. [PubMed: 24795947]
29. Nagel TM, Zitnay JL, Barocas VH, Nuckley DJ. Quantification of continuous in vivo flexion–extension kinematics and intervertebral strains. Eur Spine J. 2014; 23:754–61. [PubMed: 24487626]

30. Pearcy MJ, Tibrewal SB. Axial rotation and lateral bending in the normal lumbar spine measured by three-dimensional radiography. Spine. 1984; 9:582–7. [PubMed: 6495028]
31. Pearcy M, Portek I, Shepherd J. Three-dimensional x-ray analysis of normal movement in the lumbar spine. Spine. 1984; 9:294–7. [PubMed: 6374922]
32. Li G, Wang S, Passias P, Xia Q, Li G, Wood K. Segmental in vivo vertebral motion during functional human lumbar spine activities. Eur Spine J. 2009; 18:1013–21. [PubMed: 19301040]
33. Johannessen W, Cloyd JM, O'Connell GD, Vresilovic EJ, Elliott DM. Trans-Endplate Nucleotomy Increases Deformation and Creep Response in Axial Loading. Ann Biomed Eng. 2006; 34:687–96. [PubMed: 16482409]
34. Walter BA, Torre OM, Laudier DM, Nadich TP, Hecht AC, Iatridis JC. Form and function of the intervertebral disc in health and disease: a morphological and stain comparison study. Journal of Anatomy. 2014; 25:390–5.
35. Gruber HE, Ingram J, Hanley ENJ. An improved staining method for intervertebral disc tissue. Biotech Histochem. 2002; 77:81–3. [PubMed: 12083388]
36. Schek RM, Michalek AJ, Iatridis JC. Genipin-crosslinked fibrin hydrogels as a potential adhesive to augment intervertebral disc annulus repair. Eur Cell Mater. 2011; 21:373–83. [PubMed: 21503869]
37. Likhitpanichkul M, Dreischarf M, Illien-Junger S, Walter BA, Nukaga T, Long RG, Sakai D, Hecht AC, Iatridis JC. Fibrin-genipin adhesive hydrogel for annulus fibrosus repair: performance evaluation with large animal organ culture, in situ biomechanics, and in vivo degradation tests. Eur Cell Mater. 2014; 28:25–37. discussion37–8. [PubMed: 25036053]
38. Xia Q, Wang S, Kozanek M, Passias P, Wood K, Li G. In-vivo motion characteristics of lumbar vertebrae in sagittal and transverse planes. J Biomech. 2010; 43:1905–9. [PubMed: 20381051]
39. Pirvu T, Blanquer SBG, Benneker LM, Grijpma DW, Richards RG, Alini M, Eglin D, Grad S, Li Z. A combined biomaterial and cellular approach for annulus fibrosus rupture repair. Biomaterials. 2015; 42:11–9. [PubMed: 25542789]
40. Heuer F, Ulrich S, Claes L, Wilke H-J. Biomechanical evaluation of conventional anulus fibrosus closure methods required for nucleus replacement. Journal of Neurosurgery: Spine. 2008; 9:307–13. [PubMed: 18928230]

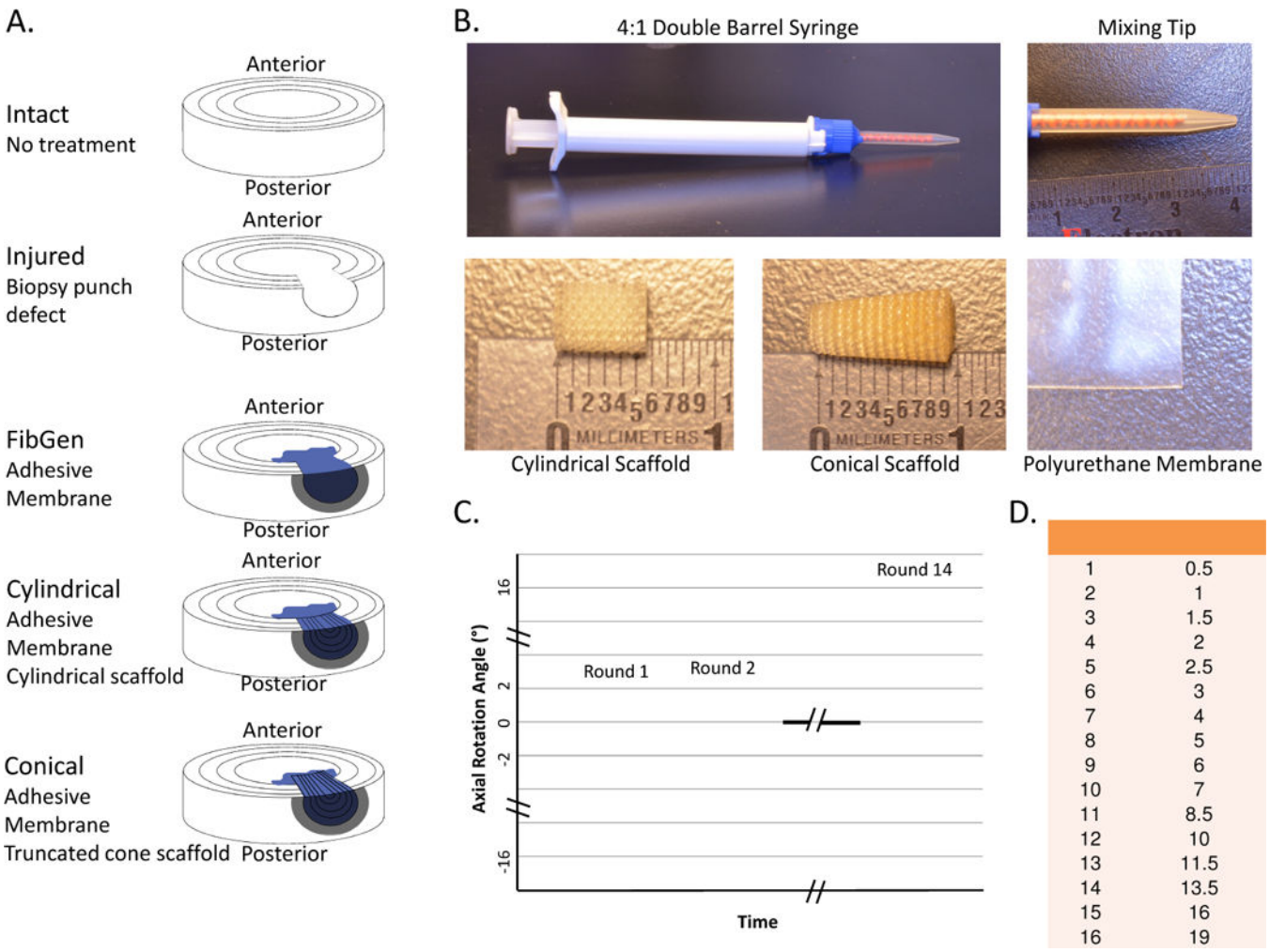

Figure 1. Part 1 Study Design

Torsion tests to determine biomechanical behaviors and herniation risk of 3 repair strategies. (A) Samples were distributed to five groups: Intact, Injured with a cylindrical biopsy punch defect, FibGen, Cylindrical scaffold and Conical (truncated cone) scaffold. Both scaffold groups also had FibGen adhesive and polyurethane membrane. (B) Individual components of the repair strategies. (C) Torsion stiffness test protocol increased torsion angle for each 'round' of 20 loading cycles. (D) Torsion angle magnitudes increased to super-physiological levels.

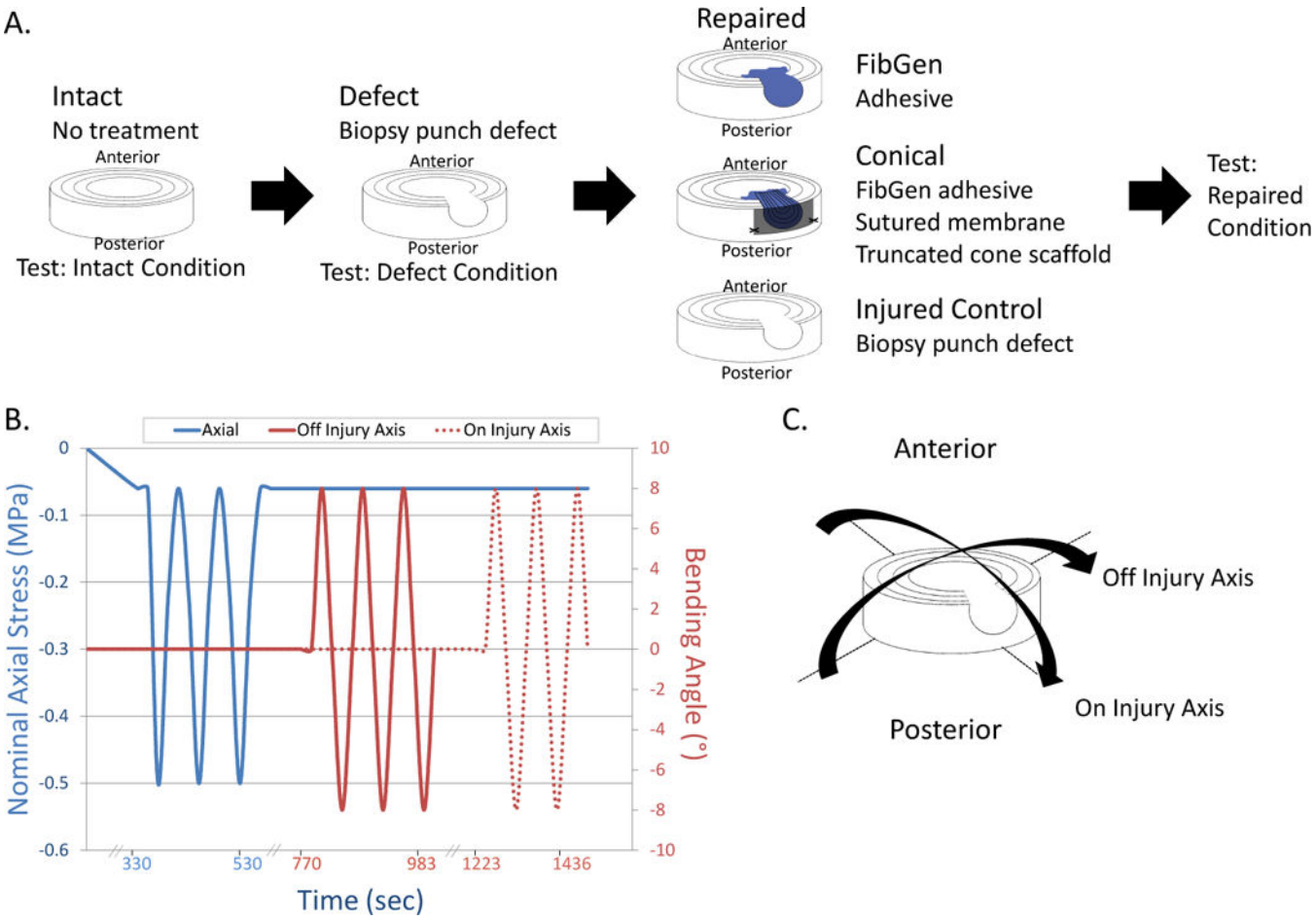

Figure 2. Part 2 Study Design

Moderate and rigorous bending stiffness tests to determine biomechanical behaviors and herniation risk of 2 repair strategies. (A) Samples were tested Intact, Injured with a cylindrical biopsy punch defect, and after being Repaired with either FibGen or a composite repair with Conical Scaffold. (B) Specimens were subjected to a bending stiffness test protocol. (C) Bending angle was applied on-axis or off-axis with the injury.

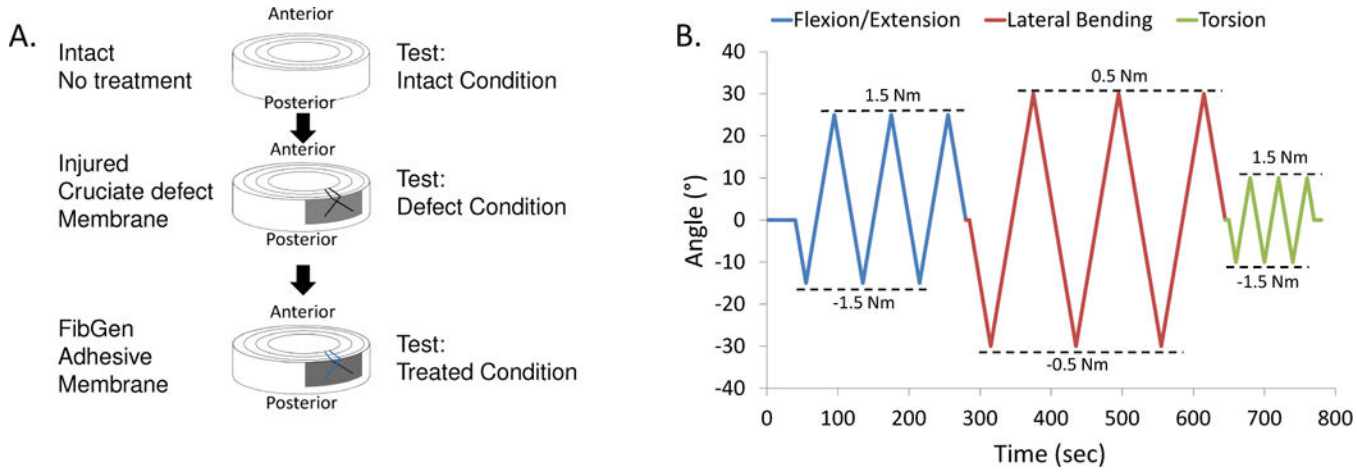

Figure 3. Part 3 Study Design

Multi-axial flexibility tests were applied to determine biomechanical behaviors of FibGen repair. (A) Samples were tested Intact, Injured with a cruciate-style defect and Repaired with FibGen. (B) Flexibility testing was performed using a constant angular velocity to a moment controlled protocol limit.

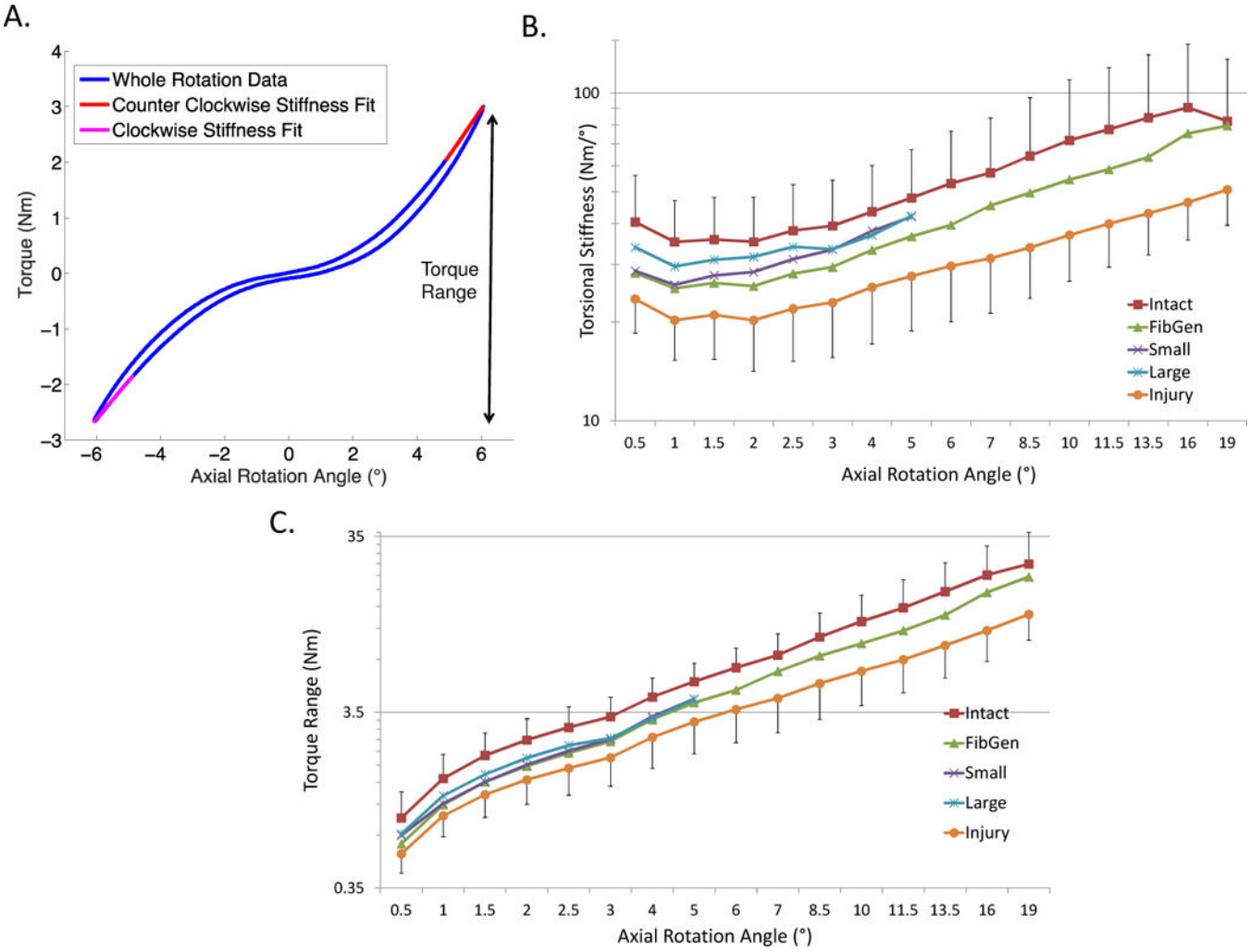

Figure 4. Part 1 Results. Torsional biomechanics

All repair strategies partially restored torsional stiffness and torque range to intact levels. (A) Torque-Rotation curves were used to calculate (B) torsional stiffness. No significant differences in torsional stiffness between groups were detected. Data presented as mean ± standard deviation. Torsional stiffness and torque range were calculated for each sample until point of extrusion so that results are only presented up to 5° for Cylindrical and Conical groups.

A.

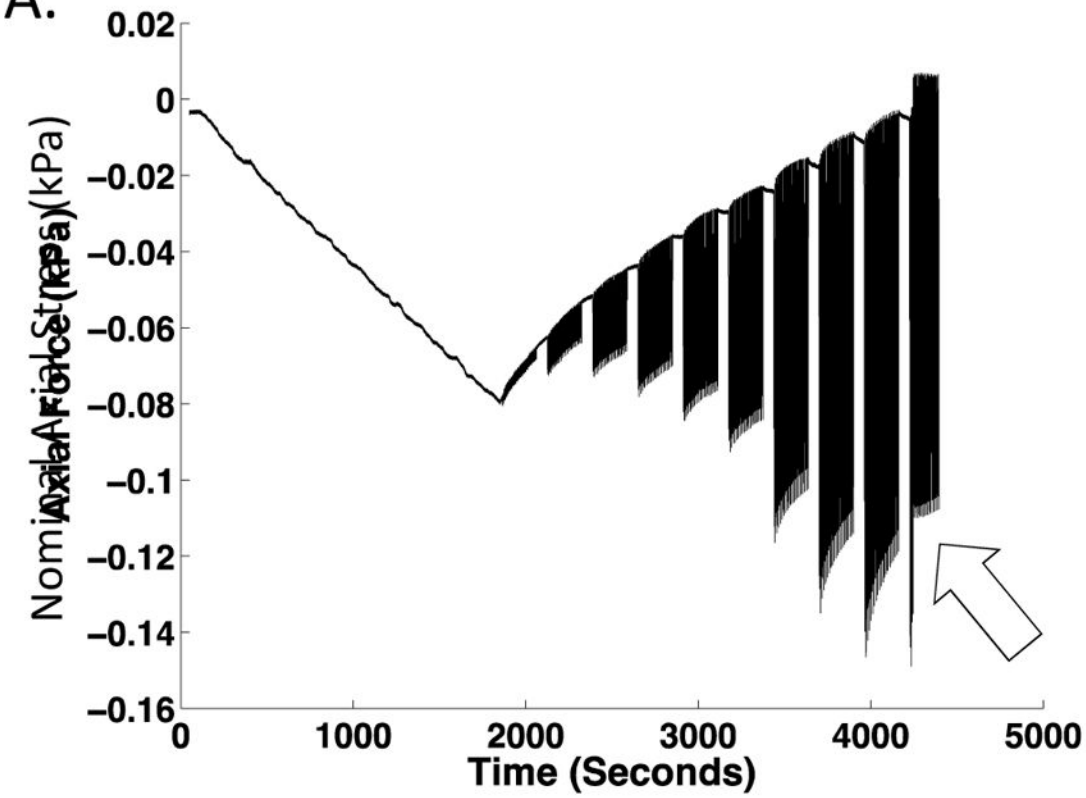

B.

Group	Max Rotation Angle (°)	Max Nominal Axial Stress (kPa)	Max Torque (Nm)	Percent Herniating (%)
Cylindrical (n=5)	6.3±2.2	320±110	3.1±0.8	100
Conical (n=6)	5.2±2.0*	320±123	3.0±1.3	83
FibGen (n=6)♯	16±5.3	610±278	10.3±5.9	33

Figure 5. Part 1 Results. Herniation biomechanics

FibGen herniated at larger rotations and torques than the scaffold based repairs and all herniated at super-physiological levels. (A) Nominal axial stress recorded during torsional loading with abrupt decrease of axial force concurrent with herniation (indicated by arrow). Maximum levels of (B) nominal axial stress, (C) rotation and (D) torque were calculated at the cycle just prior to herniation. Data presented as mean ± standard deviation. *$p<0.05$ compared to FibGen. # Means for FibGen were calculated using values at the maximum test rotation angle for the 4 FibGen samples that did not herniate so that these data under-represent failure properties for FibGen.

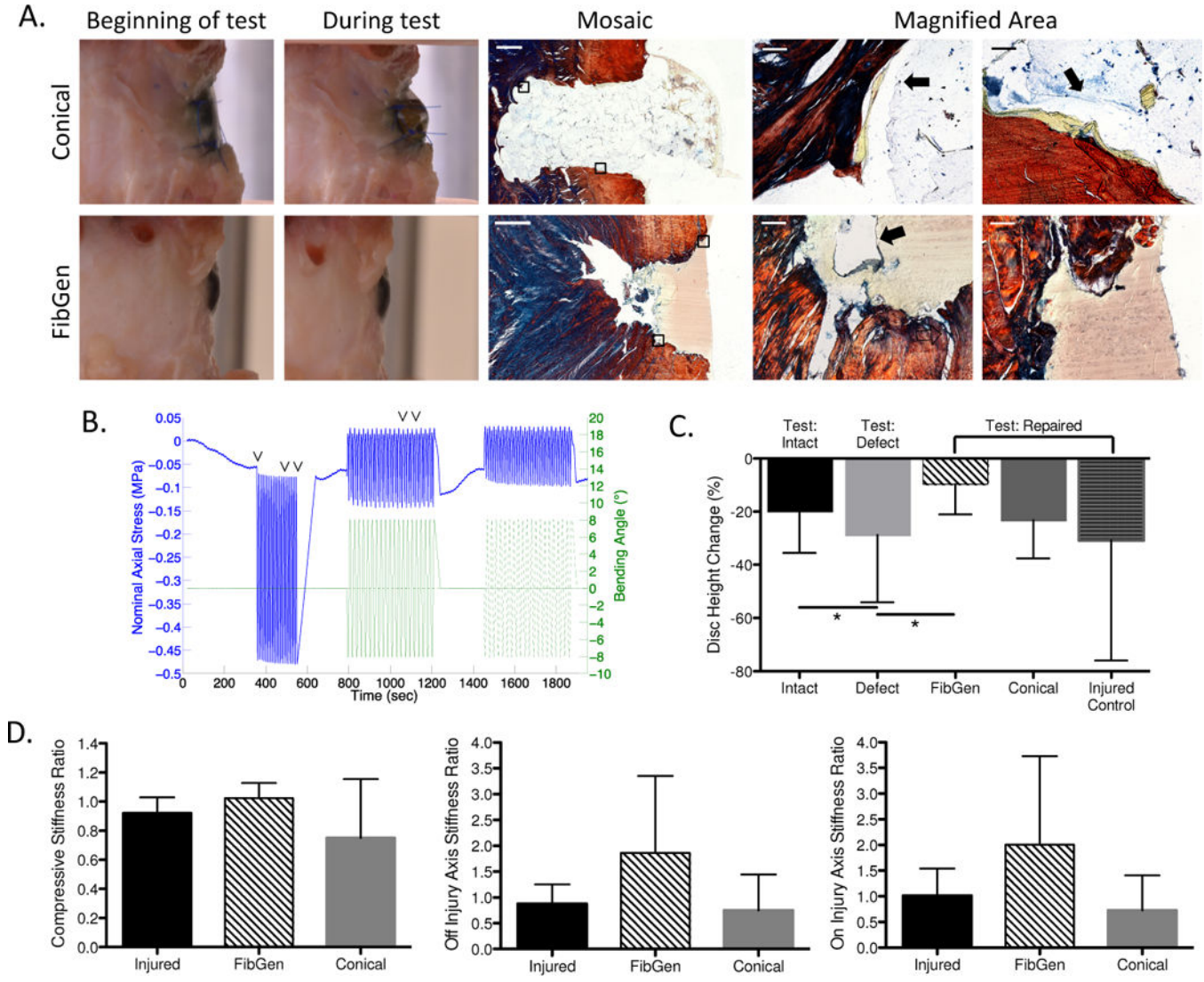

Figure 6. Part 2 Results. Herniation characterization, disc height & biomechanics

FibGen did not herniate and restored disc height while the Conical scaffold group herniated and did not restore disc height. (A) Photos and histological sections of sagittal bovine IVDs sections following repair and moderate loading for Conical samples and moderate and cyclic failure loading for FibGen. Scale bars are 1000 μm in mosaic image and 50 μm in magnified areas. For Conical group, failure occurred between Conical scaffold and FibGen (arrows, top). For FibGen group, FibGen remained adhered to the AF tissue with failure occurring by cracking of the FibGen mid-substance (black arrow) and fissuring of native disc tissue (white arrow) (bottom) (B) Axial stress and bending angle during moderate testing for characteristic sample with times of herniation for 5 of the conical scaffolds indicated (∨). (C) Disc height loss was greatest for the specimens in Defect condition and was restored for FibGen. (D) Axial and bending biomechanical results for Injured Control, FibGen and Conical scaffold groups. FibGen had the largest stiffness ratio values for all testing modes, but no significant biomechanical differences were observed with group for any stiffness ratio value. Data presented as mean ± standard deviation. *$p<0.05$.

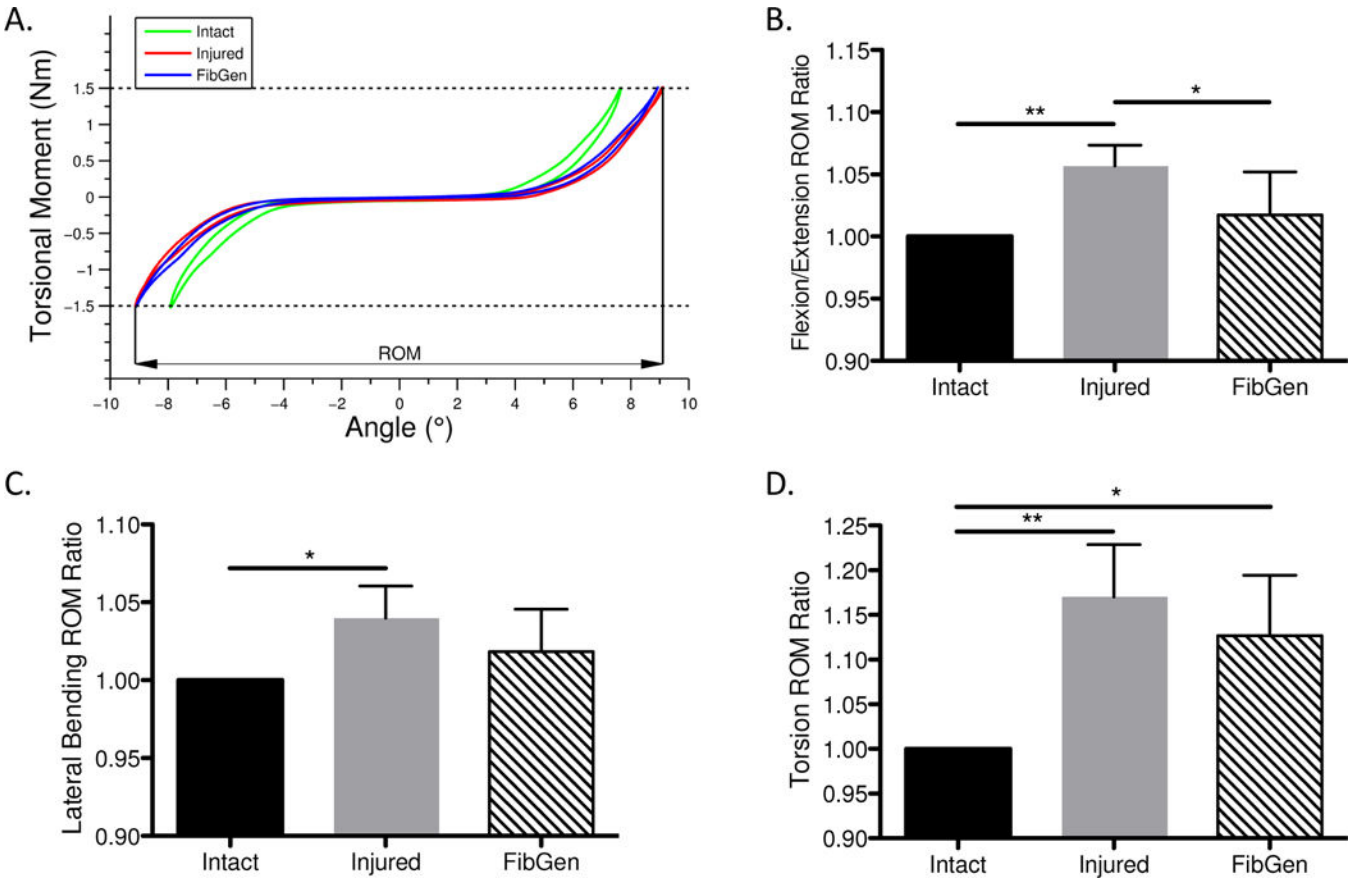

Figure 7. Part 3 Results. Multi-axial range of motion

ROM was significantly increased in the Injured group compared to Intact for all degrees of freedom. FibGen had ROM values lower than for Injured in all degress of freedom but this was only significant in flexion-extension (A) Moment and angle curves were used to calculate the ROM as the total angular motion between ±1.5Nm moment for each of the 3 rotational degrees of freedom for (B) flexion-extension, (C) lateral bending and (D) torsion. Data presented as mean ± standard deviation. *p<0.05, **p<0.01.